PAPER

An Iterative MPEG Super-Resolution with an Outer Approximation of Framewise Quantization Constraint

Hiroshi HASEGAWA[†a)], ***Member***, **Toshiyuki ONO**[††], ***Student Member***, **Isao YAMADA**[††], ***Member***, *and* **Kohichi SAKANIWA**[††], ***Fellow***

SUMMARY In this paper, we present a novel iterative MPEG super-resolution method based on an embedded constraint version of Adaptive projected subgradient method [Yamada & Ogura 2003]. We propose an efficient operator that approximates convex projection onto a set characterizing framewise quantization, whereas a conventional method can only handle a convex projection defined for each DCT coefficient of a frame. By using the operator, the proposed method generates a sequence that efficiently approaches to a solution of super-resolution problem defined in terms of quantization error of MPEG compression.

key words: *super-resolution, MPEG video, set-theoretic approach, outer approximation, adaptive projected subgradient method*

1. Introduction

The objective of super-resolution of movies is to recover underlying high-resolution images from low-resolution movies by utilizing potential redundancy [1], [2]. Because of recent widespread of HDTV system and digital video, it is newly required for super-resolution to compensate degradation caused by MPEG compression as well as to improve resolution [3]. In [4], Altunbasak et al. proposed a set-theoretic approach that can explicitly handle effect of MPEG compression. For each DCT coefficient of a frame, they defined the set of all high-resolution images satisfying a constraint on the coefficient. Then by using POCS [5], a high-resolution image satisfying all constraints is picked up from the intersection of these sets. They also showed that real-time operation can be realized by using a DSP. However, the method still has room for improvement. Firstly, the method handles an enormous number of constraint sets, where such formulation is computationally inefficient in general. Secondly, derived image suffers from noises caused by insufficient estimation owe to MPEG quantization. Finally, parallel algorithm is more desired, whereas POCS is essentially serial algorithm, because image recovery problems require huge computational load in general.

To resolve these difficulties in the above set-theoretic MPEG super-resolution, in this paper, we present a novel iterative MPEG super-resolution method based on an embedded constraint version of *Adaptive projected subgradient method* [6], [7]. At first, we define an efficient operator that approximates a convex projection onto the set of all high-resolution images satisfying a framewise quantization constraint. Then we present an MPEG super-resolution method which provides a sequence efficiently approaching to the set of all images satisfying all given constraints, where each iterative operation of the proposed method is accelerated by utilizing a property of a linear variety on which the estimation is restricted. Restriction of total variation in [8] is also introduced for denoising without corruption of edge information. Simulation result shows that the proposed method realizes resolution improvement and noise suppression as well.

A preliminary version have been presented at an international conference [9].

2. Preliminaries

2.1 Notations

Let $\mathbb{R}$ and $\mathbb{Z}$ be the set of all real numbers and integers, respectively. For all vectors $\boldsymbol{u} := (u_1, \ldots, u_{\mathcal{P}}), \boldsymbol{v} := (v_1, \ldots, v_{\mathcal{P}})$ in a $\mathcal{P}$ dimensional Euclidean space $\mathbb{R}^{\mathcal{P}}$, its inner product and induced norm are defined by $\langle \boldsymbol{u}, \boldsymbol{v} \rangle := \sum_{k=1}^{\mathcal{P}} u_k v_k$ and $\|\boldsymbol{u}\| := \sqrt{\langle \boldsymbol{u}, \boldsymbol{u} \rangle}$. A set $C \subset \mathbb{R}^{\mathcal{P}}$ is convex provided that $\forall \boldsymbol{u}, \boldsymbol{v} \in C$, $\forall \nu \in (0, 1)$, $\nu \boldsymbol{u} + (1 - \nu)\boldsymbol{v} \in C$. Given a nonempty closed convex set $C \subset \mathbb{R}^{\mathcal{P}}$, a convex projection $P_C : \mathbb{R}^{\mathcal{P}} \to C$ maps $\boldsymbol{u} \in \mathbb{R}^{\mathcal{P}}$ to the unique vector $P_C(\boldsymbol{u})$ such that $d(\boldsymbol{u}, C) := \min_{\boldsymbol{v} \in C} \|\boldsymbol{u} - \boldsymbol{v}\| = \|\boldsymbol{u} - P_C(\boldsymbol{u})\|$. For $\boldsymbol{u} := (u_1, \ldots, u_{\mathcal{P}}) \in \mathbb{R}^{\mathcal{P}}$, its m th component u_m is equivalently denoted by $\boldsymbol{u}(m)$. Let M, N, L be positive integers such that $M/8, N/8 \in \mathbb{Z}$. Suppose that we have sequences $(\boldsymbol{x}_k)_{k \in \mathbb{Z}} \subset \mathbb{R}^{L^2 MN}$ and $(\boldsymbol{y}_k)_{k \in \mathbb{Z}} \subset \mathbb{R}^{MN}$ derived through lexicographically reordering pixels of $LM \times LN$ high-resolution images and related $M \times N$ low-resolution images, respectively. Each low-resolution image is assumed to be generated by :

$$\boldsymbol{y}_k = DH_k \boldsymbol{x}_k \qquad (k \in \mathbb{Z}), \tag{1}$$

where $H_k \in \mathbb{R}^{L^2 MN \times L^2 MN}$ denotes a degradation such as blur and $D \in \mathbb{R}^{MN \times L^2 MN}$ changes resolution by averaging each $L \times L$ region. In a case of MPEG video sequences, each observed $\boldsymbol{y}_k$ is compressed by

Manuscript received August 5, 2004.
Manuscript revised May 9, 2005.
Final manuscript received June 20, 2005.
[†]The author is with the Dept. of Electrical Engineering & Computer Science, Nagoya University, Nagoya-shi, 464-8603 Japan.
[††]The authors are with the Dept. of Communications & Integrated Systems, Tokyo Institute of Technology, Tokyo, 152-8552 Japan.
a) E-mail: hasegawa@nuee.nagoya-u.ac.jp
DOI: 10.1093/ietfec/e88–a.9.2427

$$\boldsymbol{g}_k = Q\left(T(\boldsymbol{y}_k - \boldsymbol{v}_k)\right) \qquad (k \in \mathbb{Z}), \tag{2}$$

where $T \in \mathbb{R}^{MN \times MN}$ denotes 8×8 block DCT [10], $Q : \mathbb{R}^{MN} \to \mathbb{R}^{MN}$ is a quantization operator defined for $\boldsymbol{u} \in \mathbb{R}^{MN}$ by

$$(Q(\boldsymbol{u}))(m) = q_m \times \left\lfloor \frac{\boldsymbol{u}(m)}{q_m} + \frac{1}{2} \right\rfloor \quad (1 \leq m \leq MN),$$

and $\boldsymbol{v}_k$ is a low-resolution image predicted by applying motion compensation to the other special images called *key frames* [3]. If the image itself is *key frame*, $\boldsymbol{v}_k = \boldsymbol{0}$. If high compression rate is required, large value is assigned to q_m. Note that for any compression rate we have the exact value of q_m as a *priori* knowledge.

Finally, we obtain $(\boldsymbol{g}_k)_{k\in\mathbb{Z}}$ and $(\boldsymbol{v}_k)_{k\in\mathbb{Z}}$ as compressed video sequence. When the sequence is played back, we have degraded low-resolution images as follows.

$$\boldsymbol{d}_k := \boldsymbol{v}_k + T^{-1}\boldsymbol{g}_k \ \in \mathbb{R}^{MN} \qquad (k \in \mathbb{Z})$$

Hereafter, we assume that $\boldsymbol{v}_k = \boldsymbol{0}\,(k \in \mathbb{Z})$ by replacing $\boldsymbol{g}_k$ with $\boldsymbol{g}_k + T\boldsymbol{v}_k$. This modification do not affect the following discussion.

Throughout this paper, we consider next problem of MPEG super-resolution: *recover $\boldsymbol{x}_k$ from given MPEG datas $(\boldsymbol{g}_\ell)_{\ell\in\mathcal{I}_k\subset\mathbb{Z}}$ by utilizing potential redundancy.*

To denote the redundancy, we introduce the next relation, a generalization of the relation in [4], between neighboring high-resolution images:

$$\begin{aligned} \boldsymbol{x}_\ell &= B_{(\ell,k)}\boldsymbol{x}_k + G_{(\ell,k)}\boldsymbol{c}_k \\ &= [B_{(\ell,k)}\ G_{(\ell,k)}] \begin{pmatrix} \boldsymbol{x}_k \\ \boldsymbol{c}_k \end{pmatrix} \quad (\ell \in \mathcal{I}_k), \end{aligned} \tag{3}$$

where $\boldsymbol{c}_k \in \mathbb{R}^{U_k} (U_k \leq KL^2MN)$ denotes the newly introduced pixels in $(\boldsymbol{x}_\ell)_{\ell\in\mathcal{I}_k}$, and $B_{(\ell,k)} \in \mathbb{R}^{L^2MN\times L^2MN}$ and $G_{(\ell,k)} \in \mathbb{R}^{L^2MN\times U_k}$ stand for mapping of pixels between $\boldsymbol{x}_k$ and $\boldsymbol{x}_\ell$. Hereafter, as in [4], we assume that $(B_{(\ell,k)})_{\ell\in\mathcal{I}_k}$ are given or satisfactory estimated through the motion compensation. The matrices $(G_{(\ell,k)})_{\ell\in\mathcal{I}_k}$ simply stand for the components of $\boldsymbol{x}_\ell$ that have no relation with these of $\boldsymbol{x}_k$. Thus $(G_{(\ell,k)})_{\ell\in\mathcal{I}_k}$ are immediately derived as a result of the estimation of $(B_{(\ell,k)})_{\ell\in\mathcal{I}_k}$. Since $\boldsymbol{x}_k$ would be recovered from previously obtained MPEG datas $(\boldsymbol{g}_\ell)_{\ell\leq k}$, we can assume that $\ell \leq k, \forall\ell \in \mathcal{I}_k$. Then each estimation $\widehat{\boldsymbol{c}_k}$ of $\boldsymbol{c}_k$ can be obtained from previously estimated $\widehat{\boldsymbol{x}_\ell}$. In the following, we employ $\boldsymbol{x}$ and $\boldsymbol{c}$ as parameters for the sake of framewise projection that will be defined later in (7), and identify $\boldsymbol{x_c} \in \mathbb{R}^{L^2MN+U_k}$ with $(\boldsymbol{x}^T\ \boldsymbol{c}^T)^T$ for notational simplicity.

Remark 1: The conventional method in [4] assumed a relation

$$\boldsymbol{x}_\ell = A_{(\ell,k)}\boldsymbol{x}_k \qquad (\ell \in \mathcal{I}_k), \tag{4}$$

where $A_{(\ell,k)} \in \mathbb{R}^{L^2MN\times L^2MN} (\ell \in \mathcal{I}_k)$ denotes motion mapping such as transformation, and defined DCT-coefficientwise constraint sets, $\forall 1 \leq m \leq MN$,

$$C_{(\ell,k,m)} := \left\{ \boldsymbol{x} \in \mathbb{R}^{L^2MN} \,\middle|\, (TDH_\ell A_{(\ell,k)}\boldsymbol{x} - \boldsymbol{g}_\ell)(m) \in \left[-\frac{q_m}{2}, \frac{q_m}{2}\right] \right\}.$$

Then they generated a sequence $(\boldsymbol{x}_k^{(n)})_{n\geq 0}$ by

$$\boldsymbol{x}_k^{(n+1)} = P_{C_{(\ell_n,k,m_n)}}\boldsymbol{x}_k^{(n)} \tag{5}$$

where $P_{C_{(\ell,k,m)}}$ is the convex projection onto $C_{(\ell,k,m)}$ and (ℓ_n, m_n) is a circularly assigned pair of numbers in $\mathcal{I}_k \times \{1, 2, \ldots, MN\}$. The sequence converges weakly to some point in the intersection $\bigcap_{\ell\in\mathcal{I}_k, m\in\{1,\ldots,MN\}} C_{(\ell,k,m)}$. □

3. Proposed MPEG Super-Resolution with an Outer Approximation of Framewise Quantization Constraint

Next equation results from MPEG compression scheme in (2) :

$$\begin{aligned} Q\left(TDH_\ell[B_{(\ell,k)}\ G_{(\ell,k)}]\begin{pmatrix} \boldsymbol{x}_k \\ \boldsymbol{c}_k \end{pmatrix}\right) &=: Q\left(W_{(\ell,k)}\boldsymbol{x}_{\boldsymbol{c}k}\right) \\ &= \boldsymbol{g}_\ell \qquad (\ell \in \mathcal{I}_k), \end{aligned}$$

where $W_{(\ell,k)} \in \mathbb{R}^{MN\times(L^2MN+U_k)}$. For each $k \in \mathbb{Z}$ and $\ell \in \mathcal{I}_k$, we define a constraint set in terms of framewise quantization Q by

$$C_{(\ell,k)} := \left\{ \boldsymbol{x_c} \in \mathbb{R}^{L^2MN+U_k} \,\middle|\, W_{(\ell,k)}\boldsymbol{x_c} - \boldsymbol{g}_\ell \in \mathcal{HC} \right\},$$

where $\mathcal{HC} := [-\frac{q_1}{2}, \frac{q_1}{2}]\times\cdots\times[-\frac{q_{MN}}{2}, \frac{q_{MN}}{2}]$ is a hyper-cuboid. In the following, we assume that $C_{(\ell,k)} \neq \emptyset$. Closedness and convexity of $C_{(\ell,k)}$ are obvious.

Because the convex projection onto the above set requires high computational cost in general, we define an *outer approximation* $\Psi_{(\ell,k)} \subset \mathbb{R}^{L^2MN+U_k}$ of $C_{(\ell,k)}$ in terms of $\boldsymbol{x_c} \notin C_{(\ell,k)}$ (See Fig. 1) by

$$\begin{aligned} \Psi_{(\ell,k)}(\boldsymbol{x_c}) := \Big\{ \boldsymbol{u} \in \mathbb{R}^{L^2MN+U_k} \,\Big|\, &\left\langle \boldsymbol{u}, W_{(\ell,k)}^T \Delta_{(\ell,k)}^{DCT}\boldsymbol{x_c} \right\rangle \\ &\geq \left\langle P_{\boldsymbol{g}_\ell+\mathcal{HC}}\left(W_{(\ell,k)}\boldsymbol{x_c}\right), \Delta_{(\ell,k)}^{DCT}(\boldsymbol{x_c}) \right\rangle \Big\}, \end{aligned} \tag{6}$$

where $P_{\boldsymbol{g}_\ell+\mathcal{HC}} : \mathbb{R}^{MN} \to \mathbb{R}^{MN}$ is the convex projection onto hyper-cuboid $\boldsymbol{g}_\ell + \mathcal{HC} := \{\boldsymbol{g}_\ell + \boldsymbol{v} | \boldsymbol{v} \in \mathcal{HC}\}$ defined for $\boldsymbol{u} \in \mathbb{R}^{MN}$ by

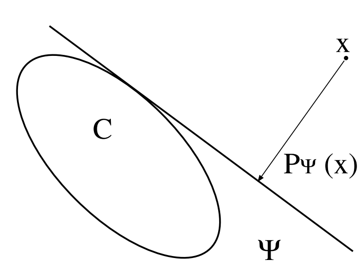

Fig. 1 An outer approximation of framewise quantization constraint and a projection onto a separating hyperplane.

$$(P_{\boldsymbol{g}_\ell + \mathcal{HC}}(\boldsymbol{u}))(m) := \begin{cases} \boldsymbol{g}_\ell(m) + \frac{q_m}{2} & \text{if } \boldsymbol{u}(m) > \boldsymbol{g}_\ell(m) + \frac{q_m}{2} \\ \boldsymbol{g}_\ell(m) - \frac{q_m}{2} & \text{if } \boldsymbol{u}(m) < \boldsymbol{g}_\ell(m) - \frac{q_m}{2} \\ \boldsymbol{u}(m) & \text{otherwise,} \end{cases}$$

and $\Delta^{DCT}_{(\ell,k)} : \mathbb{R}^{L^2MN+U_k} \to \mathbb{R}^{MN}$ such that

$$\Delta^{DCT}_{(\ell,k)}(\boldsymbol{x_c}) := P_{\boldsymbol{g}_\ell + \mathcal{HC}}(W_{(\ell,k)}\boldsymbol{x_c}) - W_{(\ell,k)}\boldsymbol{x_c}.$$

The convex projection of $\boldsymbol{x_c} \notin C_{(\ell,k)}$ onto $\Psi_{(\ell,k)}(\boldsymbol{x_c})$ is nothing but the orthogonal projection onto the boundary of $\Psi_{(\ell,k)}(\boldsymbol{x_c})$. Since the boundary separates $\boldsymbol{x_c}$ and $\Psi_{(\ell,k)}(\boldsymbol{x_c})$, it is called *separating hyperplane*. The convex projection provides an operator that efficiently approximates the convex projection onto $C_{(\ell,k)}$.

$$P_{\Psi_{(\ell,k)}(\boldsymbol{x_c})}(\boldsymbol{x_c}) := \begin{cases} \boldsymbol{x_c} & \text{if } \boldsymbol{x_c} \in C_{(\ell,k)}, \\ \boldsymbol{x_c} + \dfrac{\left\|\Delta^{DCT}_{(\ell,k)}(\boldsymbol{x_c})\right\|^2}{\left\|W^T_{(\ell,k)}\Delta^{DCT}_{(\ell,k)}(\boldsymbol{x_c})\right\|^2} W^T_{(\ell,k)}\Delta^{DCT}_{(\ell,k)}(\boldsymbol{x_c}) & \text{otherwise} \end{cases} \quad (7)$$

Remark 2:

1. In more general case where two Hilbert spaces and a linear operator, that is a mapping from one space to the other, are given, an outer approximation can be given as in (6) (See Appendix A).
2. If rank $(W_{(\ell,k)}) = MN$, namely the matrix being full row rank, the assumption $C_{(\ell,k)} \neq \emptyset$ is justified. Moreover, in such a case, the boundary of $\Psi_{(\ell,k)}(\boldsymbol{x_c})$ and $C_{(\ell,k)}$ have a nonempty intersection. Then the boundary of $\Psi_{(\ell,k)}(\boldsymbol{x_c})$ becomes a *supporting hyperplane*. (See Corollary 1 in Appendix A)
3. As for the efficiency of the proposed operator, see Appendix B □

Next constraint is necessary to handle the additional parameter $\boldsymbol{c}$ of $\boldsymbol{x_c}$.

$$V_k := \left\{ \boldsymbol{x_c} = \begin{pmatrix} \boldsymbol{x} \\ \boldsymbol{c} \end{pmatrix} \in \mathbb{R}^{L^2MN+U_k} \;\middle|\; \boldsymbol{c} = \widehat{\boldsymbol{c}}_k \right\}$$

Let $\mathcal{M}_k := \{(\boldsymbol{x}^T\, \boldsymbol{0}^T)^T | \boldsymbol{x} \in \mathbb{R}^{L^2MN}\} \subset \mathbb{R}^{L^2MN+U_k}$ be a linear subspace parallel to the linear variety V_k. The convex projection onto $\mathcal{M}_k$ is $P_{\mathcal{M}_k}(\boldsymbol{x_c}) := (\boldsymbol{x}^T\, \boldsymbol{0}^T)^T$.

Additionally we introduce a restriction in total variation which efficiently suppresses noise while keeping edge information [8]. The constraint set is defined for given threshold $\sigma_{\text{tv}}(\geq 0)$ by

$$C_{\text{tv}} := \left\{ \boldsymbol{x_c} \in \mathbb{R}^{L^2MN+U_k} \;\middle|\; \text{tv}(\boldsymbol{x}) - \sigma_{\text{tv}} \leq 0 \right\},$$

where $\text{tv} : \mathbb{R}^{L^2MN} \to \mathbb{R}$ is the total variation given by (See [8, Eq. (12)])

$$\begin{aligned} \text{tv}(\boldsymbol{x}) :=& \sum_{p=1}^{LM-1}\sum_{q=1}^{LN-1} \{|x(p+1,q) - x(p,q)|^2 \\ &+ |x(p,q+1) - x(p,q)|^2\}^{1/2} \\ &+ \sum_{p=1}^{LM-1} |x(p+1,LN) - x(p,LN)| \\ &+ \sum_{q=1}^{LN-1} |x(LM,q+1) - x(LM,q)| \\ =:& \sum_{p=1}^{LM-1}\sum_{q=1}^{LN-1} \|\Gamma_{(p,q)}\boldsymbol{x}\| + \sum_{p=1}^{LM-1} |\Gamma_{(p,LN)}\boldsymbol{x}| \\ &+ \sum_{q=1}^{LN-1} |\Gamma_{(LM,q)}\boldsymbol{x}| \end{aligned}$$

with difference matrices $(\Gamma_{(p,q)})_{1\leq p\leq LM-1, 1\leq q\leq LN-1} \subset \{-1, 0, 1\}^{2\times L^2MN}$, $(\Gamma_{(p,LN)})_{1\leq p\leq LM} \subset \{-1,0,1\}^{1\times L^2MN}$, $(\Gamma_{(LM,q)})_{1\leq q\leq LN} \subset \{-1,0,1\}^{1\times L^2MN}$, and (p,q) th pixel $x(p,q) := \boldsymbol{x}((p-1)LN + q)$. It is also shown that an outer approximation $\Psi_{\text{tv}}(\boldsymbol{x_c}) \subset \mathbb{R}^{L^2MN+U_k}$ can be given as a halfspace, satisfying $C_{\text{tv}} \subset \Psi_{\text{tv}}(\boldsymbol{x_c})$,

$$\Psi_{\text{tv}}(\boldsymbol{x_c}) := \begin{cases} \left\{ \boldsymbol{x} \in \mathbb{R}^{L^2MN+U_k} \mid \langle \boldsymbol{x_c} - \boldsymbol{x}, \boldsymbol{t} \rangle \geq \text{tv}(\boldsymbol{x_c}) - \sigma \right\} & \text{if } \boldsymbol{x_c} \notin C_{\text{tv}} \\ \mathbb{R}^{L^2MN+U_k} & \text{otherwise,} \end{cases}$$

where $\boldsymbol{t}$ is a selection of subgradient, which is given by

$$\boldsymbol{t} := \sum_{p=1}^{LM-1}\sum_{q=1}^{LN-1} u_{(p,q)} + \sum_{p=1}^{LM-1} u^{(h)}_{(p,LN)} + \sum_{q=1}^{LN-1} u^{(v)}_{(LM,q)}$$

with

$$u_{(p,q)} := \begin{cases} 0 & \text{if } \Gamma_{(p,q)}\boldsymbol{x} = \boldsymbol{0} \\ \Gamma^T_{(p,q)}\Gamma_{(p,q)}\boldsymbol{x}/\|\Gamma_{(p,q)}\boldsymbol{x}\| & \text{otherwise} \end{cases}$$

$$u^{(h)}_{(p,LN)} := \begin{cases} 0 & \text{if } \Gamma_{(p,LN)}\boldsymbol{x} = \boldsymbol{0} \\ \Gamma^T_{(p,LN)}\Gamma_{(p,LN)}\boldsymbol{x}/|\Gamma_{(p,LN)}\boldsymbol{x}| & \text{otherwise} \end{cases}$$

$$u^{(v)}_{(LM,q)} := \begin{cases} 0 & \text{if } \Gamma_{(LM,q)}\boldsymbol{x} = \boldsymbol{0} \\ \Gamma^T_{(LM,q)}\Gamma_{(LM,q)}\boldsymbol{x}/|\Gamma_{(LM,q)}\boldsymbol{x}| & \text{otherwise.} \end{cases}$$

Then *subgradient projection* $P_{\Psi_{\text{tv}}(\boldsymbol{x_c})} : \mathbb{R}^{L^2MN+U_k} \to \mathbb{R}^{L^2MN+U_k}$, that is an economical approximation of $P_{C_{\text{tv}}}$ is given by

$$P_{\Psi_{\text{tv}}(\boldsymbol{x_c})} := \begin{pmatrix} \boldsymbol{v} \\ \boldsymbol{c} \end{pmatrix}$$

with

$$\boldsymbol{v} := \begin{cases} \boldsymbol{x} - \dfrac{(\text{tv}(\boldsymbol{x}) - \sigma)\boldsymbol{t}}{\|\boldsymbol{t}\|^2} & \text{if } \text{tv}(\boldsymbol{x}) > \sigma \\ \boldsymbol{x} & \text{otherwise.} \end{cases}$$

Finally, the set of all $\boldsymbol{x_c}$ satisfying given constraints is characterized as $(\bigcap_{\ell\in\mathcal{I}_k} C_{(\ell,k)}) \cap C_{\text{tv}} \cap V_k$. We assume

$(\bigcap_{\ell \in \mathcal{I}_k} C_{(\ell,k)}) \cap C_{\mathrm{tv}} \cap V_k \neq \emptyset$. This assumption would be justified especially when large value is assigned q_m to achieve high compression rate, because q_m controls the volume of each $C_{(\ell,k)}$ and large q_m means broad $C_{(\ell,k)}$. Application of an embedded constraint version of *Adaptive projected subgradient method* (See [7, Example 5]) generates a sequence efficiently approaching to the intersection.

Algorithm 1: For any $\boldsymbol{x}_{\boldsymbol{c}_k}^{(0)} \in V_k$, generate a sequence $(\boldsymbol{x}_{\boldsymbol{c}_k}^{(n)})_{n \geq 0} \subset \mathbb{R}^{L^2MN+U_k}$ by the following equation

$$\boldsymbol{x}_{\boldsymbol{c}_k}^{(n+1)} := \begin{cases} \boldsymbol{x}_{\boldsymbol{c}_k}^{(n)} & \text{if } \Theta_n'\left(\boldsymbol{x}_{\boldsymbol{c}_k}^{(n)}\right) \in \mathcal{M}_k^{\perp} \\ \boldsymbol{x}_{\boldsymbol{c}_k}^{(n)} - \lambda_n \dfrac{\Theta_n\left(\boldsymbol{x}_{\boldsymbol{c}_k}^{(n)}\right)}{\left\| P_{\mathcal{M}_k}\left(\Theta_n'\left(\boldsymbol{x}_{\boldsymbol{c}_k}^{(n)}\right)\right)\right\|^2} & \\ \qquad \times P_{\mathcal{M}_k}\left(\Theta_n'\left(\boldsymbol{x}_{\boldsymbol{c}_k}^{(n)}\right)\right) & \text{otherwise,} \end{cases}$$

where $\lambda_n \in [0, 2]$ and

$$\Theta_n(\boldsymbol{x}_{\boldsymbol{c}}) := \sum_{t=0}^{K-1} w_t d\left(\boldsymbol{x}_{\boldsymbol{c}}, \Psi_{(\ell_t,k)}(\boldsymbol{x}_{\boldsymbol{c}_k}^{(n)})\right) + w_K d\left(\boldsymbol{x}_{\boldsymbol{c}}, \Psi_{\mathrm{tv}}(\boldsymbol{x}_{\boldsymbol{c}_k}^{(n)})\right)$$

$$\Theta_n'(\boldsymbol{x}_{\boldsymbol{c}}) := \sum_{t=0}^{K-1} w_t \frac{\boldsymbol{x}_{\boldsymbol{c}} - P_{\Psi_{(\ell_t,k)}(\boldsymbol{x}_{\boldsymbol{c}_k}^{(n)})}(\boldsymbol{x}_{\boldsymbol{c}})}{\left\|\boldsymbol{x}_{\boldsymbol{c}} - P_{\Psi_{(\ell_t,k)}(\boldsymbol{x}_{\boldsymbol{c}_k}^{(n)})}(\boldsymbol{x}_{\boldsymbol{c}})\right\|} + w_K \frac{\boldsymbol{x}_{\boldsymbol{c}} - P_{\Psi_{\mathrm{tv}}(\boldsymbol{x}_{\boldsymbol{c}_k}^{(n)})}(\boldsymbol{x}_{\boldsymbol{c}})}{\left\|\boldsymbol{x}_{\boldsymbol{c}} - P_{\Psi_{\mathrm{tv}}(\boldsymbol{x}_{\boldsymbol{c}_k}^{(n)})}(\boldsymbol{x}_{\boldsymbol{c}})\right\|}$$

with $\mathcal{I}_k =: \{\ell_0, \ldots, \ell_{K-1}\}$ and $(w_t)_{t=0}^{K}$ such that $w_t \geq 0$ and $\sum_{t=0}^{K} w_t = 1$.

Remark 3:

1. Algorithm 1 has a *Monotone approximation* property [7, Theorem 2]. Namely, $\forall \lambda_n \in (0, 2)$, $\|\boldsymbol{u} - \boldsymbol{x}_{\boldsymbol{c}_k}^{(n+1)}\| < \|\boldsymbol{u} - \boldsymbol{x}_{\boldsymbol{c}_k}^{(n)}\|$ holds for $\forall \boldsymbol{u} \in \bigcap_{\ell \in \mathcal{I}_k} C_{(\ell,k)} \cap C_{\mathrm{tv}} \cap V_k$. (For further discussion about the convergence, see [6])
2. Since efficiency of algorithm is important as in statement 2 of Remark 2, V_k is embedded so that $P_{\mathcal{M}_k}$ accelerates the update.
3. At each step of Algorithm 1, a weighted average of the projections is used to generate the sequence. Therefore the projections can be computed independently, and the proposed method can be executed on parallel processing systems.

4. Numerical Example

We generate two distinct MPEG datas $(\boldsymbol{g}_k)_{k=1}^{20}$, by downsampling and compression of original high-resolution images $(\boldsymbol{x}_k)_{k=1}^{20}$. The original high-resolution images are obtained by clipping out from given grayscale still pictures. All pixels in $\boldsymbol{x}_k$ shift, relative to $\boldsymbol{x}_{k-1}$, from bottom-right to top-left by (1,2) (k:even) or (2,1) (k:odd).

In practical MPEG compression scheme the quantization intervals are dynamically changed so that generated stream satisfies given bitrates, and different types of key frames exist. However, for simplicity, in this section we employ a simplified compression scheme with fixed quantization intervals. Key frames are 1, 6, 11, 16 th frames and we employ pixelwise motion estimations. For each 8×8 region, the quantization interval q_m at (p, q) th position is given by $2^{\lfloor (p+q-1)/2 \rfloor}$ $(1 \leq p, q \leq 8)$. The matrices $(H_k)_{k=1}^{20}, (B_{(\ell,k)})_{(\ell,k) \in \{\mathbb{Z} \cap [1,20]\}^2}, (D_{(\ell,k)})_{(\ell,k) \in \{\mathbb{Z} \cap [1,20]\}^2}$ are assumed to be exactly estimated. Let $\mathrm{tv}_{\mathrm{org}}$ be total variation of each original image to be recovered. Then the proposed method is applied to the following two examples.

Example 1: The sequence of the original images is generated from a grayscale picture, a short range view (Main gate of Tokyo Institute of Technology) with $M = 144, N = 96, L = 2, \mathcal{I}_k = \{k, k-1, \ldots, k-7\}$ $(k = 8, 9, \ldots, 20)$. For blurring, we applied a two dimensional Gaussian filter with variance 20 that is truncated to 5×5 and normalized. The original image $\boldsymbol{x}_{20}$ and the compressed image are shown in Figs. 2(a) and (b), respectively. The threshold of total variation σ_{tv} is determined so that we can suppress the quantization noise. Because the compressed images already lose the information of high-frequency components partially, the threshold must be smaller than the original value $\mathrm{tv}_{\mathrm{org}}$ to derive denoising effect. If there is no blur, namely $H_k = I$ $(k \in \mathbb{Z})$, it seems that $\sigma_{\mathrm{tv}} = 0.8 \times \mathrm{tv}_{\mathrm{org}}$ gives good result for the quantization interval. (After 160 iterations, we have a result in Fig. 2(c)).

Because of the low-pass characteristic of the Gaussian filter, the information of high-frequency components is severely degraded after quantization, and the inverse of the filter tends to enhance errors of high-frequency components. In this case, the recovered images in Figs. 2(d) and (e) are derived after 160 iterations. Because of the loss of high-frequency components, the recovered images are slightly degraded compared with Fig. 2(c), and smaller threshold $\sigma_{\mathrm{tv}} = 0.75 \times \mathrm{tv}_{\mathrm{org}}$ gives better result.

For comparison we applied a POCS based method that is straightforwardly derived by generalizing the relation in (5) between $\boldsymbol{x}_k$ and $\boldsymbol{x}_\ell$ from (4) to (3) :

$$\boldsymbol{x}_{\boldsymbol{c}_k}^{(n+1)} = P_{V_k} P_{C_{(\ell_n,k,MN)}} P_{C_{(\ell_n,k,MN-1)}} \cdots P_{C_{(\ell_n,k,1)}} \boldsymbol{x}_{\boldsymbol{c}_k}^{(n)} \quad (n \geq 0)$$

where ℓ_n is circularly assigned number in $\mathcal{I}_k$. The numbers of frames processed in each iteration of the proposed method and the POCS based method are different. However, parallel processing systems are now becoming popular in these days, and the proposed method can assign each projection onto the outer approximation to each processor of the system.

After 160 iterations, we have the image in Fig. 2(f). Quantization noises are found around edges whereas they are suppressed in Figs. 2(d) and (e). The wave-like noises, caused by estimation error in the previous frame, at the bottom and the right hand side of Fig. 2(f) are more severe than than these of Figs. 2(d) and (e). This improvement owes to

(a) Original high-resolution image.

(b) Compressed low-resolution image. (PSNR=29.02 dB)

(c) Proposed with $\sigma_{\text{tv}} = 0.8 \times \sigma_{\text{org}}$ without blur. (PSNR=33.19 dB)

(d) Proposed with $\sigma_{\text{tv}} = 0.75 \times \sigma_{\text{org}}$. (PSNR=31.75 dB)

(e) Proposed with $\sigma_{\text{tv}} = 0.8 \times \sigma_{\text{org}}$. (PSNR=31.45 dB)

(f) Conventional. (PSNR=30.42 dB)

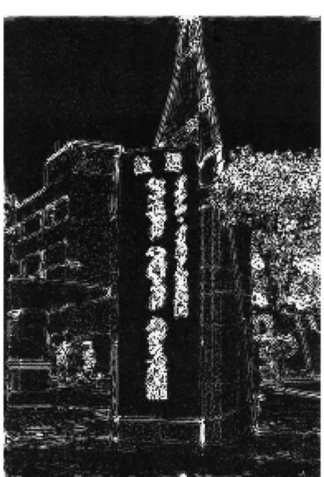

(g) Difference between (a) and (d).

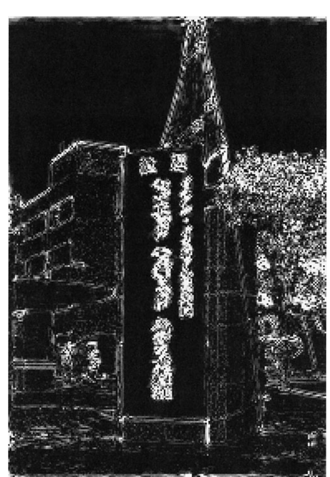

(h) Difference between (a) and (e).

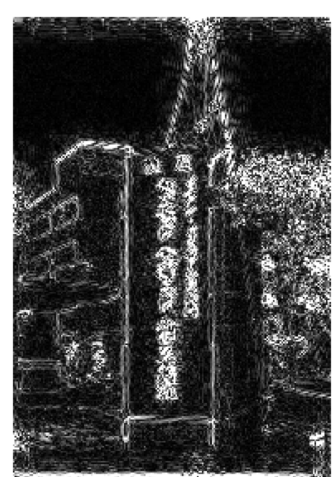

(i) Difference between (a) and (f).

Fig. 2 A short range view (Main gate of Tokyo Institute of Technology).

(a) Original high-resolution image.

(b) Compressed low-resolution image. (PSNR=30.29 dB)

(c) Proposed with $\sigma_{\rm tv} = 0.8 \times \sigma_{\rm org}$. (PSNR=36.07 dB)

(d) Conventional. (PSNR=35.52 dB)

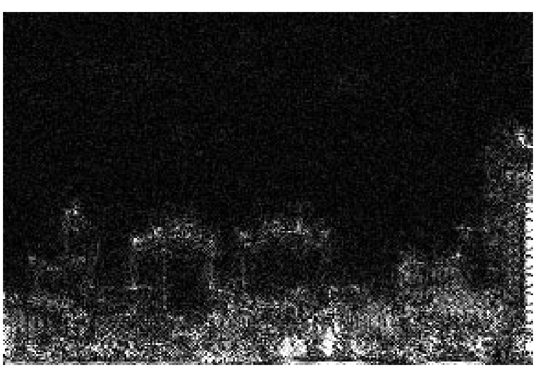

(e) Difference between (a) and (c).

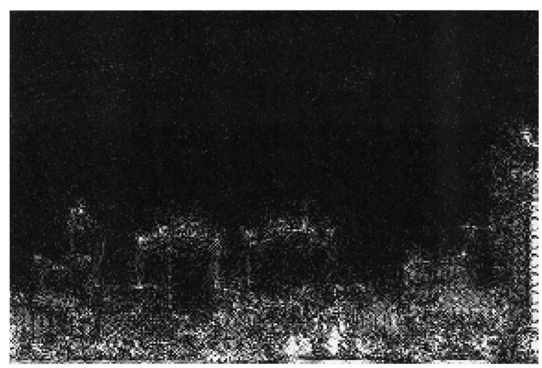

(f) Difference between (a) and (d).

Fig. 3 A distant view (Tokyo Bay).

the restriction on total variation where such a constraint is impossible to introduce to the conventional method. The PSNRs also show that the proposed method improves the quality of the recovered image.

The difference to the original images are illustrated in Figs. 2(g), (h), and (i). They shows $10 \times \mathrm{abs}(\boldsymbol{x}_{20} - \widehat{\boldsymbol{x}_{20}})$ where $\widehat{\boldsymbol{x}_{20}}$ is the derived image and abs is a operator that computes absolute value of each component of given vector. The factor 10 is introduced only to enhance the difference. We can also verify that the proposed method especially suppresses the quantization noise around edges.

Example 2: The sequence of the original images is generated from a grayscale picture, a distant view (Tokyo Bay) with $M = 96, N = 144, L = 2, \mathcal{I}_k = \{k, k-1, \ldots, k-7\}$ ($k = 8, 9, \ldots, 20$). Here we assume that H_k is an identity matrix (no blur). In this case, the sequential projections of POCS realize maximum efficiency (See Appendix B).

The threshold is fixed to $\sigma_{\rm tv} = 0.8 \times \mathrm{tv}_{\rm org}$. We have the images in Figs. 3(c) and (d) after 80 iterations of the proposed method and the POCS based method, respectively. The difference to the original images are also illustrated in Figs. 3(e) and (f). They demonstrates that the denoising effect of the proposed method around edges. The PSNRs also show that the proposed method improves the quality of the recovered image.

5. Conclusion

In this paper, we proposed an operator that efficiently approximates a convex projection onto the framewise constraint set. Then we also proposed a MPEG super-resolution method based on the Adaptive projected subgradient method, where each iterative operation is consisted of the proposed operators and is accelerated by utilizing a property that one of constraint sets becomes a linear variety.

Acknowledgment

The authors would like to express deep gratitude to Dr. N. Ogura at Musashi Institute of Technology for his valuable comments and advises, and Prof. K. Sato at Nagoya University for his kind support.

References

[1] S.C. Park, M.K. Park, and M.G. Kang, "Super-resolution image reconstruction—A technical overview," IEEE Signal Process. Mag., vol.20, no.3, pp.21–36, May 2003.
[2] M.K. Ng and N.K. Bose, "Mathematical analysis of super-resolution methodology," IEEE Signal Process. Mag., vol.20, no.3, pp.62–74, May 2003.
[3] C.A. Segall, R. Molina, and A.K. Katsaggelos, "High-resolution images from low-resolution compressed video," IEEE Signal Process. Mag., vol.20, no.3, pp.37–48, May 2003.
[4] Y. Altunbasak, A.J. Patti, and R.M. Mersereau, "Super-resolution still and video reconstruction from MPEG-coded video," IEEE Trans. Circuits Syst. Video Technol., vol.12, no.4, pp.217–226, April 2002.
[5] H. Stark and Y. Yang, Vector space projections—A numerical approach to signal and image processing, neural nets, and optics, John Wiley & Sons, 1998.
[6] I. Yamada and N. Ogura, "Adaptive projected subgradient method and its applications to set theoretic adaptive filtering," Proc. 37th Asilomar Conference on Signals, Systems and Computers, pp.600–607, Nov. 2003.
[7] I. Yamada and N. Ogura, "Adaptive projected subgradient method for asymptotic minimization of sequence of nonnegative convex functions," Numerical Functional Analysis and Optimization, vol.25, no.7&8, pp.593–617, 2004.
[8] P.L. Combettes and J.-C. Pesquet, "Image restoration subject to a total variation constraint," IEEE Trans. Image Process., vol.13, no.9, pp.1213–1222, Sept. 2004.
[9] H. Hasegawa, T. Ono, I. Yamada, and K. Sakaniwa, "An iterative MPEG super-resolution with an outer approximation of framewise quantization constraint," Proc. 6th IEEE International Workshop on Multimedia Signal Processing, Pw1-6, Sept. 2004.
[10] W.K. Pratt, Digital Image Processing, 2nd ed., John Wiley & Sons, 1991.

Appendix A: A Scheme to Derive an Outer Approximation

Let $\mathcal{H}_1$ and $\mathcal{H}_2$ be Hilbert spaces with inner products $\langle\cdot,\cdot\rangle_1, \langle\cdot,\cdot\rangle_2$ and induced norms $\|\boldsymbol{x}\|_1 := \sqrt{\langle \boldsymbol{x},\boldsymbol{x}\rangle_1}\,(\boldsymbol{x} \in \mathcal{H}_1)$, $\|\boldsymbol{y}\|_2 := \sqrt{\langle \boldsymbol{y},\boldsymbol{y}\rangle_2}\,(\boldsymbol{y} \in \mathcal{H}_2)$, respectively. Let $L : \mathcal{H}_1 \to \mathcal{H}_2$ be a bounded linear operator with $L^* : \mathcal{H}_2 \to \mathcal{H}_1$ satisfying $\langle L\boldsymbol{x},\boldsymbol{y}\rangle_2 = \langle \boldsymbol{x}, L^*\boldsymbol{y}\rangle_1\,(\boldsymbol{x} \in \mathcal{H}_1, \boldsymbol{y} \in \mathcal{H}_2)$. Suppose that $C' \subset \mathcal{H}_2$ be a nonempty closed convex set and $C := \{\boldsymbol{x} \in \mathcal{H}_1 \,|\, L\boldsymbol{x} \in C'\}$. If $C' \neq \emptyset$, C is also closed and convex because of boundedness of L. We assume that C' is simple enough to give an explicit expression of convex projection $P_{C'} : \mathcal{H}_2 \to C'$. For arbitrary fixed $\boldsymbol{x}_0 \in \mathcal{H}_1$, we define a set $V(\boldsymbol{x}_0)$ by

$$V(\boldsymbol{x}_0) := \{\boldsymbol{x} \in \mathcal{H}_1 \,|\, \langle L\boldsymbol{x} - L\boldsymbol{x}_0, P_{C'}(L\boldsymbol{x}_0) - L\boldsymbol{x}_0\rangle_2 = \|P_{C'}(L\boldsymbol{x}_0) - L\boldsymbol{x}_0\|_2^2\}. \quad \text{(A· 1)}$$

Lemma 1: $V(\boldsymbol{x}_0)$ in (A· 1) is a hyperplane in $\mathcal{H}_1$. □

Proof: For any $\boldsymbol{v} \in V(\boldsymbol{x}_0)$, we have

$$\begin{aligned}&\langle \boldsymbol{v} - \boldsymbol{x}_0, L^*(P_{C'}(L\boldsymbol{x}_0) - L\boldsymbol{x}_0)\rangle_1\\ &= \langle L(\boldsymbol{v} - \boldsymbol{x}_0), P_{C'}(L\boldsymbol{x}_0) - L\boldsymbol{x}_0\rangle_2\\ &= \|P_{C'}(L\boldsymbol{x}_0) - L\boldsymbol{x}_0\|_2^2.\end{aligned}$$

The above equation shows that $V(\boldsymbol{x}_0)$ is a hyperplane. (Q.E.D.)

Let a halfspace $H^-(\boldsymbol{x}_0)$ be

$$H^-(\boldsymbol{x}_0) := \{\boldsymbol{x} \in \mathcal{H}_1 \,|\, \langle L\boldsymbol{x} - L\boldsymbol{x}_0, P_{C'}(L\boldsymbol{x}) - L\boldsymbol{x}_0\rangle_2 \geq \|P_{C'}(L\boldsymbol{x}) - L\boldsymbol{x}_0\|_2^2\}. \quad \text{(A· 2)}$$

We call $V(\boldsymbol{x}_0)$ a *separating hyperplane* when $\boldsymbol{x}_0 \notin H^-(\boldsymbol{x}_0)$ and $C \subset H^-(\boldsymbol{x}_0)$. If $C \cap H^-(\boldsymbol{x}_0) \neq \emptyset$, $V(\boldsymbol{x}_0)$ is specially called *supporting hyperplane*.

Theorem 1: For arbitrary fixed $\boldsymbol{x}_0 \notin C$, $V(\boldsymbol{x}_0)$ in (A· 1) is a separating hyperplane. □

Proof: Since $L\boldsymbol{x}_0 \notin C'$, we have $P_{C'}(L\boldsymbol{x}_0) \neq L\boldsymbol{x}_0$ and

$$\langle L\boldsymbol{x}_0 - L\boldsymbol{x}_0, P_{C'}(L\boldsymbol{x}_0) - L\boldsymbol{x}_0\rangle_2 = 0 < \|P_{C'}(L\boldsymbol{x}_0) - L\boldsymbol{x}_0\|_2^2. \quad \text{(A· 3)}$$

On the other hand, for any $\boldsymbol{y} \in C'$, $\boldsymbol{y} = \{\boldsymbol{y} - P_{C'}(L\boldsymbol{x}_0)\} + P_{C'}(L\boldsymbol{x}_0)$. Because $P_{C'}$ is a convex projection, it holds that

$$\langle \boldsymbol{y} - P_{C'}(L\boldsymbol{x}_0), P_{C'}(L\boldsymbol{x}_0) - L\boldsymbol{x}_0\rangle_2 \geq 0.$$

Hence, if there exists $\boldsymbol{x} \in \mathcal{H}_1$ such that $\boldsymbol{y} = L\boldsymbol{x}$, we have

$$\begin{aligned}&\langle \boldsymbol{y} - L\boldsymbol{x}_0, P_{C'}(L\boldsymbol{x}_0) - L\boldsymbol{x}_0\rangle_2\\ &= \langle \{\boldsymbol{y} - P_{C'}(L\boldsymbol{x}_0)\} + \{P_{C'}(L\boldsymbol{x}_0) - L\boldsymbol{x}_0\},\\ &\qquad P_{C'}(L\boldsymbol{x}_0) - L\boldsymbol{x}_0\rangle_2\\ &= \langle \boldsymbol{y} - P_{C'}(L\boldsymbol{x}_0), P_{C'}(L\boldsymbol{x}_0) - L\boldsymbol{x}_0\rangle_2\\ &\qquad + \|L\boldsymbol{x}_0 - P_{C'}(L\boldsymbol{x}_0)\|_2^2\\ &\geq \|L\boldsymbol{x}_0 - P_{C'}(L\boldsymbol{x}_0)\|_2^2.\end{aligned} \quad \text{(A· 4)}$$

Eqs. (A· 3) and (A· 4) shows that $V(\boldsymbol{x}_0)$ is a separating hyperplane. (Q.E.D.)

The next corollary is straightforward.

Corollary 1: $V(\boldsymbol{x}_0)$ in Eq. (A· 1) is a supporting hyperplane when $P_{C'}(L\boldsymbol{x}_0)$ is included in the range of L. □

Finally, we have a convex projection onto $V(\boldsymbol{x}_0)$, which is easy to compute and is an economical approximation to the convex projection onto C.

(a) Projection onto the proposed outer approximation. (PSNR=28.02 dB)

(b) A cycle of sequential projections onto pixelwise constraint sets. (PSNR = 27.56 dB)

Fig. A· 1 Image recovery from single observed image with limited number of operations.

Appendix B: Efficiency of the Proposed Operator

Since only small number of iterations is available in real-time applications, efficiency of each iteration is important. A measure of such an efficiency would be the ratio between the distances to given set before/after the operation. Unfortunately the exact distance to the framewise constraint set $C_{(\ell,k)}$ is hard to compute. Thus we employ the distance in DCT domain or PSNR, a function of distance to the original image, as measures of the efficiency.

For simplicity, suppose that $\mathcal{I}_k = \{k\}$. In this case we have $U_k = 0$ and the dimension of $\boldsymbol{c}_k$ is zero. In a special case that $H_\ell = I$ (no blur), the sequential projection of the conventional method $P_{C_{(\ell,k,MN)}} P_{C_{(\ell,k,MN-1)}} \cdots P_{C_{(\ell,k,1)}}$ provides the exact projection onto the framewise constraint set $C_{(\ell,k)}$ because the DCT operator T is an orthogonal transform and the row vectors of D are orthogonal to each other. However their orthogonality are not valid if $H_\ell \neq I$ and the efficiency of the proposed method is verified by the following experiments.

- Let $\boldsymbol{g}_k \in \mathbb{R}^{64\times 64}$ be an MPEG data that is obtained from a 128×128 grayscale photo of the sky. Suppose that H_k stands for a normalized uniform 2-D Gaussian blur with zero-mean and variance 20. We employ $\|\Delta^{DCT}_{(k,k)}(\cdot)\|$, which denotes distance in DCT domain to $C_{(k,k)}$, as a measure of efficiency of each iteration. For randomly generated 100 high-resolution images $(\boldsymbol{x}^{(n)})_{n=1}^{100}$, we compute ensemble averages of (i)$\|\Delta^{DCT}_{(k,k)}(\boldsymbol{x}^{(n)})\|$ for the original points, (ii)$\|\Delta^{DCT}_{(k,k)}(P_{\Psi_{(k,k)}(\boldsymbol{x}^{(n)})}(\boldsymbol{x}^{(n)}))\|$ for the proposed operator, (iii)$\|\Delta^{DCT}_{(k,k)}(P_{(k,k,MN)} \cdots P_{(k,k,1)}(\boldsymbol{x}^{(n)}))\|$ for cyclic application of the conventional projection. Then a ratio of (ii) to (i) is 0.107, whereas the ratio of (iii) to (i) is 0.394.
- We applied the proposed operator and a cycle of the sequential projection of POCS based method to the image $\boldsymbol{x}_1$ of the Example 1. After the result of 20 iterative operations of the proposed method, we have images in Fig. A· 1. Because only one image is employed for recovery and severe blurring is applied, the quality of the images are not satisfactory. However, the Euclidean distance to the original image is reduced to 3367.7 (PSNR=28.02 dB) whereas that by the POCS based method is 3552.2 (PSNR=27.56 dB). Note that the distances to the constraint set are smaller than these values.

NOTE: We also tested with the other images and the proposed operator always realizes better PSNRs for all images.

Hiroshi Hasegawa received the B.E., M.E., and D.E. degrees all in Electrical and Electronic Engineering from Tokyo Institue of Technology, Tokyo, Japan, in 1995, 1997, and 2000, respectively. From 2000 to 2005, he was a research associate of Dept. of Communications and Integrated Systems, Tokyo Institute of Technology. Currently he is an associate professor of Nagoya University. His current research interests include Photonic Networks, Image Processing (especially Super-resolution), Multidimensional Digital Signal Processing and Time-Frequency Analysis. He received the Young Researcher Awards from SITA (Society of Information Theory and its Applications) and IEICE (Institute of Electronics, Information and Communication Engineers) in 1993 and 1995, respectively. Dr. Hasegawa is a member of SITA and IEEE.

Toshiyuki Ono received the B.E. degree from Tokyo Institute of Technology in 2004. He is currently pursuing the M.E. degree in Department of Communications and Integrated Systems at Tokyo Institute of Technology. His research interest includes Digital Signal Processing and Image Processing, especially adaptive processing of Super-Resolution Image Recovery.

Isao Yamada received the B.E. degree in computer science in 1985 from University of Tsukuba, and the M.E. and Ph.D. degrees in Electrical and Electronic Engineering from Tokyo Institute of Technology, in 1987 and 1990, respectively. Currently he is an associate professor in the Department of Communications and Integrated Systems at Tokyo Institute of Technology. He received the Excellent Paper Awards, in 1990 and 1994, and the Young Researcher Award, in 1992, from IEICE and the ICF Research Award, in 2004, from the International Communications Foundation (ICF). Dr. Yamada is a member of the IEEE, AMS, SIAM and SITA.

Kohichi Sakaniwa received B.E., M.E., and Ph.D. degrees all in electronic engineering from the Tokyo Institute of Technology, Tokyo Japan, in 1972, 1974 and 1977, respectively. He joined the Tokyo Institute of Technology in 1977 as a research associate and served as an associate professor from 1983 to 1991. Since 1991 he has been a professor in the Department of Electrical and Electronic Engineering, and since 2000 in the Department of Communication and Integrated Systems, Graduate School of Science and Engineering, both in the Tokyo Inst. of Tech. From November 1987 to July 1988, he stayed at the University of Southwestern Louisiana as a Visiting Professor. He received the Excellent Paper Award from the IEICE of Japan in 1982, 1990, 1992 and 1994. His research area includes Communication Theory, Error Correcting Coding, (Adaptive) Digital Signal Processing and so on. Dr. Sakaniwa is a member of IEEE, Information Processing Society of Japan, Institute of Image Information and Television Engineers of Japan, and Society of Information Theory and its Applications.